International Communications in Heat and Mass Transfer 45 (2013) 41–46

Contents lists available at SciVerse ScienceDirect

International Communications in Heat and Mass Transfer

journal homepage: www.elsevier.com/locate/ichmt

Estimation of turbulent natural convection in horizontal parallel plates by the Q criterion ☆

Wu-Shung Fu *, Yu-Chih Lai, Chung-Gang Li

Department of Mechanical Engineering, National Chiao Tung University, Hsinchu 30010, Taiwan

ARTICLE INFO

Available online 29 April 2013

Keywords:
Turbulent natural convection
Q criterion
Numerical simulation
Parallel plates

ABSTRACT

An investigation of estimation of turbulent structures of natural convection in horizontal parallel plates by the Q criterion is studied numerically. It is difficult to adopt a definite criterion like the critical Reynolds number adopted in forced convection to distinguish laminar and turbulent flows of natural convection in horizontal parallel plates because the angle between directions of the buoyancy force and main stream flow is changed in the whole process of the flowing. The Q criterion is then used to make up for a deficiency of the definite criterion and examines mechanisms of the occurrence of rotation behaviors which are often regarded as turbulent structures in detail. Methods of the Roe scheme, preconditioning and dual time stepping matching the method of LUSGS are simultaneously used to solve a low speed compressible flow. As well, non-reflecting boundary conditions are held at apertures to prevent the reflection caused by pressure waves. Under a low height situation, the shear force is dominant, and then a few rotation behaviors are observed near the central region where flow directions are changed. Oppositely, the space is almost filled with active rotation behaviors because natural convection fully develops in a high height situation.

1. Introduction

Until now a turbulent channel flow caused by forced [1–5] or natural [6–11] convection is still a very important subject for both academic and industrial research. The most apparent characteristics of the turbulent flow are generally recognized as that the Reynolds number of the flow is larger than the critical Reynolds number of the flow and numerous active eddy behaviors are observed in the flow. Therefore, based upon the criterion of the critical Reynolds number the attribution of a situation of forced convection channel flow, in which the mass flow rate of the channel flow is a given condition, can be easily predicted whether it belongs to a turbulent flow or not. An appropriate solution method for the force convection channel flow can be correctly adopted accompanied with the prediction mentioned above.

However, under a situation of natural convection the mass flow rate is mainly induced by both thermal and geometric conditions, and it has difficulty to assign the mass flow rate as a given condition in advance like the situation of forced convection. Also, the buoyancy force, which is produced by a variation of the density of the fluid because of different heating locations, is a driving force and a function of a heating location that leads different velocities of fluids to be induced in the flow. As a result, observation of the mixture of laminar and turbulent natural convections in the flow becomes possible due to the mixture of low and high velocities of fluids mentioned above. As well, under horizontal parallel plates directions of the buoyancy force and main stream flow are vertical in regions near the inlet and outlet, and parallel in near central regions [12]. Then the angle between both directions of the buoyancy force and main stream flow is alternatively changed in the situation of horizon parallel plates that causes a definitely critical criterion similar to the critical Reynolds number proposed to distinguish laminar and turbulent flows of natural convection to be difficult. Related numerical and theoretic studies for investigating turbulent natural convection in the situation of horizontal parallel plates are scarcely published.

For investigating turbulent natural convection in the horizontal parallel plates further, the study aims to investigate eddy behaviors of turbulent natural convection in the horizontal parallel plates by a method of the Q-criterion [13] numerically. The lateral width is elongated five times as long as that of [12] to get rid of restriction of eddy behaviors. Derived finite differential formulae are advanced to a higher order than those used in [12] for catching sensitive eddy behaviors clearly. The Q-criterion [13] can indicate locations of the rotation which can be regarded as a kind of eddy behavior in the flow. Based upon the results, the flow inclines to a turbulent or laminar flow can be objectively observed. For considering a situation including variable buoyancy forces induced by variable densities of fluids, the compressibility of the fluid is taken into consideration. Methods of the Roe scheme [14], preconditioning [15], and dual time stepping matching [15] the LUSGS method [16] are simultaneously adopted to solve a compressible flow. The results show that under a situation of the high modified Rayleigh number the space for developing natural convection is large, and then active behaviors of the rotation are very apparent. This phenomenon indicates

☆ Communicated by W.J. Minkowycz.

* Corresponding author at: Department of Mechanical Engineering, National Chiao Tung University, 1001 Ta Hsueh Road, Hsinchu, 30010, Taiwan.
E-mail address: wsfu@mail.nctu.edu.tw (W.-S. Fu).

0735-1933/$ – see front matter © 2013 Elsevier Ltd. All rights reserved.
http://dx.doi.org/10.1016/j.icheatmasstransfer.2013.04.001

Nomenclature

e	internal energy (J/kg)
g	acceleration of gravity (m/s^2)
H	height of the plate (m)
J	Jacobian
k	thermal conductivity (W/mK)
k_0	surrounding thermal conductivity (W/mK)
Nu_x	local Nusselt number defined in Eq. (36)
	$Nu_{x_1} = \frac{H}{k_0(T_h - T_c)}\left[k(T)\frac{\partial T}{\partial x_2}\right]$
$\overline{Nu}$	area average local Nusselt number defined in Eq. (37)
	$\overline{Nu} = \frac{1}{4W^2}\int_0^W Nu_{x_1} dx_3$
P	pressure (Pa)
P_0	surrounding pressure (Pa)
Pr	Prandtl number
Q	Q-criterion defined in Eq. (33) $Q = -\frac{1}{2}(S_{ij}S_{ij} - \Omega_{ij}\Omega_{ij})$
R	gas constant (J/kg/K)
Ra	Rayleigh number defined in Eq. (34) $Ra = \Pr\frac{g\rho_0^2(T_h - T_c)H^3}{T_0\mu(T)^2}$
Ra^*	modified Rayleigh number defined in Eq. (35) $Ra^* = Ra \times \frac{4W}{H}$
t	physical times (s)
T	temperature (K)
T_0	temperature of surroundings (K)
T_h	temperature of heat surface (K)
u_1,u_2,u_3	velocities in x_1, x_2 and x_3 directions (m/s)
W	width of the plate (m)
x_1,x_2,x_3	Cartesian coordinates (m)

Greek symbols

α	thermal diffusivity rate (m^2/s)
ρ	density (kg/m^3)
ρ_0	surrounding density (kg/m^3)
μ	viscosity (N·s/m^2)
γ	specific heat ratio
τ	artificial times
ξ, η, ζ	curvilinear coordinate

the flow field filled with turbulence structures, and becomes a fully unstable situation. Oppositely, under a situation of the low modified Rayleigh number the space for developing natural convection is contracted, except near central regions behaviors of the rotation are scarcely observed. Fluids usually turn directions in near central regions, and a few indicators of the rotation are then observed.

2. Physical model

A physical model of three dimensional horizontal parallel plates is indicated in Fig. 1. The length, height and width are 4 W, H and W, respectively. Compared with the previous study [12], the width is much wider because the turbulence structures in the spanwise direction (x_3) should be taken into consideration as well as those in the other two directions. The temperature of the heated bottom surface is T_h (700 K), and the top plate is adiabatic. The gravity is downward and the temperature and pressure of surroundings are T_0 (298 K) and P_0 (101,300 Pa), respectively. Boundary conditions on both apertures are non-reflecting conditions and both sides of the width are periodic conditions.

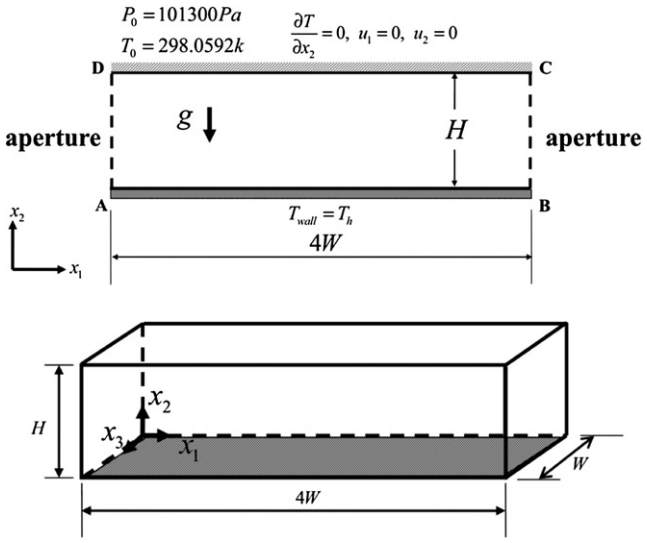

Fig. 1. Physical model.

For facilitating the analysis, the following assumptions are made.

1. The work fluid is ideal gas and follows the equation of state of an ideal gas.
2. Magnitudes of gradients of density and pressure on the whole surfaces in the normal direction are zero.

3. Radiation heat transfer is neglected

The governing equations in which the parameters of viscosity and compressibility of the fluid and gravity are simultaneously considered are shown in the following equations.

$$\frac{\partial U}{\partial t} + \frac{\partial F_1}{\partial x_1} + \frac{\partial F_2}{\partial x_2} + \frac{\partial F_3}{\partial x_3} = S \tag{1}$$

$$P = \rho RT \tag{2}$$

The quantities included in U and F_i are separately shown in the following equations.

$$U = \begin{pmatrix} \rho \\ \rho u_1 \\ \rho u_2 \\ \rho u_3 \\ \rho e \end{pmatrix} \tag{3}$$

and

$$F_i = \begin{pmatrix} \rho u_i \\ \rho u_i u_1 + P\delta_{i1} - \mu A_{i1} \\ \rho u_i u_2 + P\delta_{i2} - \mu A_{i2} \\ \rho u_i u_3 + P\delta_{i3} - \mu A_{i3} \\ (\rho e + P)u_i - \mu A_{ij}u_j - k\frac{\partial T}{\partial x_i} \end{pmatrix}, \forall i = 1,\ 2,\ 3 \tag{4}$$

where $A_{ij} = \frac{\partial u_j}{\partial x_i} + \frac{\partial u_i}{\partial x_j} - \frac{2}{3}(\nabla \cdot u)\delta_{ij}$.

$$S = \begin{pmatrix} 0 \\ 0 \\ -(\rho - \rho_0)g \\ 0 \\ -(\rho - \rho_0)gu_2 \end{pmatrix}. \tag{5}$$

The viscosity and thermal conductivity of the fluid are based upon Sutherland's law

$$\mu(T) = \mu_0 \left(\frac{T}{T_0}\right)^{\frac{3}{2}} \frac{T_0 + 110}{T + 110}, \tag{6}$$

$$k(T) = \frac{\mu(T)\gamma R}{(\gamma - 1)\mathrm{Pr}}, \tag{7}$$

where $\rho_0 = 1.1842\ \mathrm{kg/m^3}$, $\mu_0 = 1.85 \times 10^{-5}\ \mathrm{N{\cdot}s/m^2}$, $T_0 = 298.0592\ K$, $\gamma = 1.4$, $R = 287\ \mathrm{J/kg/K}$, and $\mathrm{Pr} = 0.72$.

4. Numerical method

The numerical method used to solve flow, thermal and pressure fields of this study is based on the previous studies of [12] and [17].

One of the main purposes in the present study is to observe the turbulence structures by Q-criterion [13]. The Q-criterion is defined as follows

$$Q = -\frac{1}{2}\left(S_{ij}S_{ij} - \Omega_{ij}\Omega_{ij}\right) \tag{8}$$

where

$$S_{ij} = \frac{1}{2}\left(\frac{\partial u_i}{\partial x_j} + \frac{\partial u_j}{\partial x_i}\right) = Sym\left(\frac{\partial u_i}{\partial x_j}\right) \quad and$$

$$\Omega_{ij} = \frac{1}{2}\left(\frac{\partial u_i}{\partial x_j} - \frac{\partial u_j}{\partial x_i}\right) = Asym\left(\frac{\partial u_i}{\partial x_j}\right).$$

When the magnitude of the Q-criterion is positive, the rotation is dominant and overcomes the strain and shear. Thus, those surfaces will be eligible as a vortex envelopes. Because the vorticity close to the center of the vortex should increase, the Q is naturally expected to remain a positive magnitude in the core of the vortex. Therefore, positive regions of the Q are good indicators of turbulent structures.

5. Results and discussion

The height H of parallel plates is generally regarded as a characteristic length when the Rayleigh number is used in parallel plate problems and defined as follows.

$$Ra = \mathrm{Pr}\frac{g\rho_0{}^2(T_h - T_c)H^3}{T_0\mu(T)^2} \tag{9}$$

However, the length of the heated bottom wall affects heat transfer phenomena remarkably. In order to highlight the influence of the length of the heated wall, a modified Rayleigh number Ra^* is newly defined in the following equation.

$$Ra^* = Ra \times \frac{4W}{H} \tag{10}$$

In the present study, two different heights which are H, named case A, and $0.5H$, named case B, are adopted to observe the effects of the heights on the formation of the rotation calculated by [13]. The modified Rayleigh numbers based on the H and $0.5H$ as the characteristic lengths are 6×10^6 and 1.5×10^6, respectively. The definitions of an instantaneous local Nusselt number at $x_3 = W/2$ and an area-averaged Nusselt number are expressed as follows, respectively.

$$Nu_{x_1} = \frac{H}{k_0(T_h - T_c)}\left[k(T)\frac{\partial T}{\partial x_2}\right] \tag{11}$$

$$\overline{Nu} = \frac{1}{4W^2}\int_0^W \int_0^{4W} Nu_{x_1}\, dx_1\, dx_3 \tag{12}$$

In Fig. 2, grid distributions in the x_1x_2 plane for case A and case B are shown, respectively. In order to capture the accurate phenomena, the grids near the wall are a little strengthened. Other parameters which are used in calculations are tabulated in Table 1. Comparing with [12], the grid number in x_3 direction is increased to 50, which can obtain the turbulent structures accurately. Δx_{2f} indicates the distance between the first grid point and the wall.

Shown in Fig. 3, area-averaged Nusselt numbers of cases of A and B are indicated by solid and dashed lines, respectively. Both cases are under a quasi-steady situation. Because the space of case A for the development of natural convection is much larger than that of case B, then area-averaged Nusselt numbers of case A are naturally larger than those of case B.

In Fig. 4, figures of a thermal field, velocity vectors and instantaneous local Nusselt numbers of cases A and B at a certain instant are revealed, respectively. Since the height of case A is high, it easily causes natural convection to be more active and unstable [12]. A convex high temperature region close to the central region is observed remarkably, and near the left side of the central region a relatively small convex high temperature region is observed. This phenomenon is mainly caused by two large circulation zones distributed on both sides of the center line. The convex high temperature region leads velocity vectors of fluids to be upward hurriedly and violently. Upward velocity vectors of fluids in the opposite region are then suppressed and indicate relatively weak behaviors. Due to accumulation of heat energy on the two convex high temperature regions, the smallest averaged Nusselt number is then found out in one of these regions. Two large circulations mutually squeeze that leads unforeseen large Nusselt numbers to be observed in the middle region.

In case B, the height is low and the space for the development of natural convection is contracted. Therefore, complicated phenomena similar to those of case A are no longer observed. Cooling fluids sucked from surroundings are orderly and sequentially heated by the heated bottom surface and begin to flow upward near the central region. Afterward, cooling fluids impinge the top surface and turn flow directions to surroundings. This situation is relatively stable, and then the smallest magnitudes of the thermal field, velocity vectors and instantaneous local Nusselt numbers are found out in the central region.

Traditionally, behaviors of the vortex which can be equivalently expressed by motions of the rotation are often regarded as turbulence structures. And the quantitative magnitude of the rotation can be estimated by the Q-criterion [13] and calculated by Eq. (8) mentioned above. Fig. 5 reveals indicators of the iso-surface of the Q of cases of A and B, respectively. The instant is the same as that of Fig. 4, and the magnitude of the iso-surface Q is equal to 500 calculated by Eq. (8). The formation of the iso-surface of the Q validates the width in the x_3 direction to be suitable for developing complete flow structures. In case A, the high height provides more active behaviors of natural convection. As well, fluids heated by the heated bottom surface flow upward near the low central region and turn flow directions close to the upper central region. As a result, a large number of lumps of the iso-surface of the Q are observed around the central region. As heated fluids flow away from the central region to surroundings, the number of lumps of the iso-surface of the Q is decreased abruptly. This phenomenon implies, in addition to the monotonous flow direction of fluids in this region, an achievement of the influence of the shear force caused by the top surface on fluid flows to be gained.

Fluids sucked from surroundings first flow through low regions of entrances into the domain. Accompanying with the heating process, these fluids flow along the bottom surface and reach the central

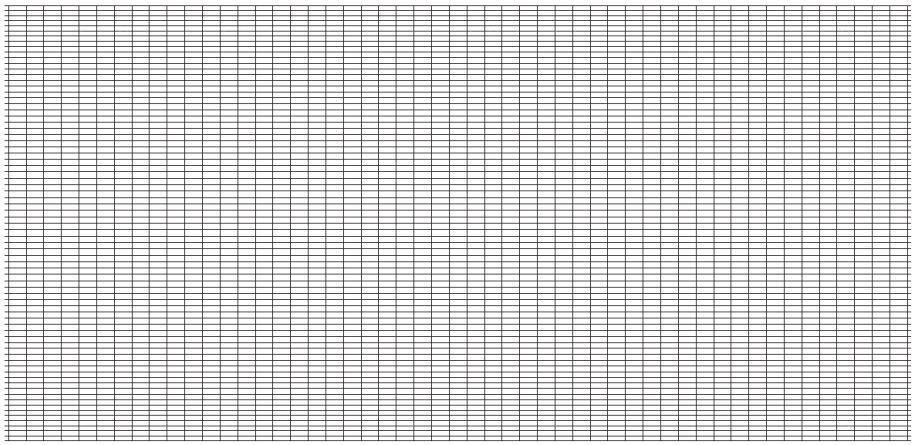

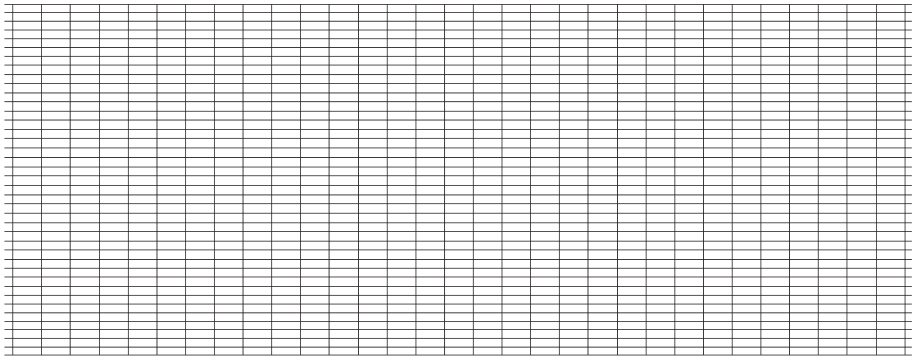

Fig. 2. Grid distribution in x_1x_2 plane.

region around. These entrance regions are approximately surrounded by dashed lines and shown in case A. Due to the dominance of suction effect, directions of fluids are almost straight in these regions that directly cause the formation of the rotation of fluid flows to have difficulty. Therefore, no lump of the iso-surface of Q is observed in these regions.

In case B, the height is low and the shear force becomes strong that seriously limits the development of natural convection in the domain. Fluids sucked from surroundings begin to flow upward close to the low central region and flow outward near the upper central region. The variation of the flow direction causes the rotation of fluid flow to happen and lumps of the iso-surface of the Q to be naturally found out in these regions. As for the other regions, due to the strong shear force the lump of the iso-surface of the Q is hardly found out.

In Fig. 6, distributions of the magnitude of lumps of the iso-surface of the Q equaling to 300 of cases A and B are indicated, respectively. The magnitude shown in this figure is smaller than that of Fig. 5 that means behaviors of the rotation shown in this figure is not active as those shown in Fig. 5. As a result, in case A both distributions of lumps of the iso-surface of the Q of Figs. 5 and 6 have no apparent difference due to the relatively complete development of natural convection. However, the behavior of the smaller magnitude of the iso-surface of the Q is relatively remarkable in the low height space, so the distribution of the small magnitude of lumps of the iso-surface of the Q shown in Fig. 6 case B is apparently denser than that of the large magnitude of lumps of the iso-surface of the Q shown in Fig. 5 case B.

Oppositely, in Fig. 7 the magnitude of lumps of the iso-surface of the Q broadly increases to 1000. The larger magnitude means the behavior to be more active. Naturally, the cluster of lumps of the iso-surface of the Q shown in this figure is more dispersed than those shown in Figs. 5 and 6.

Table 1
Cases parameters.

Case	Domain size(m)	Grid numbers	$\Delta x_1 \times \Delta x_{2f} \times \Delta x_3$ (m)
A	$0.02 \times 0.05 \times 0.05$	$200 \times 75 \times 50$	$0.002 \times 0.000276 \times 0.01$
B	$0.02 \times 0.025 \times 0.05$	$200 \times 40 \times 50$	$0.002 \times 0.000289 \times 0.01$

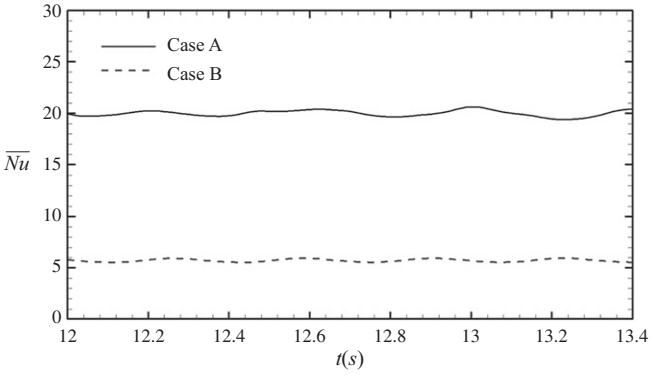

Fig. 3. Variations of time and space averaged Nusselt numbers with time.

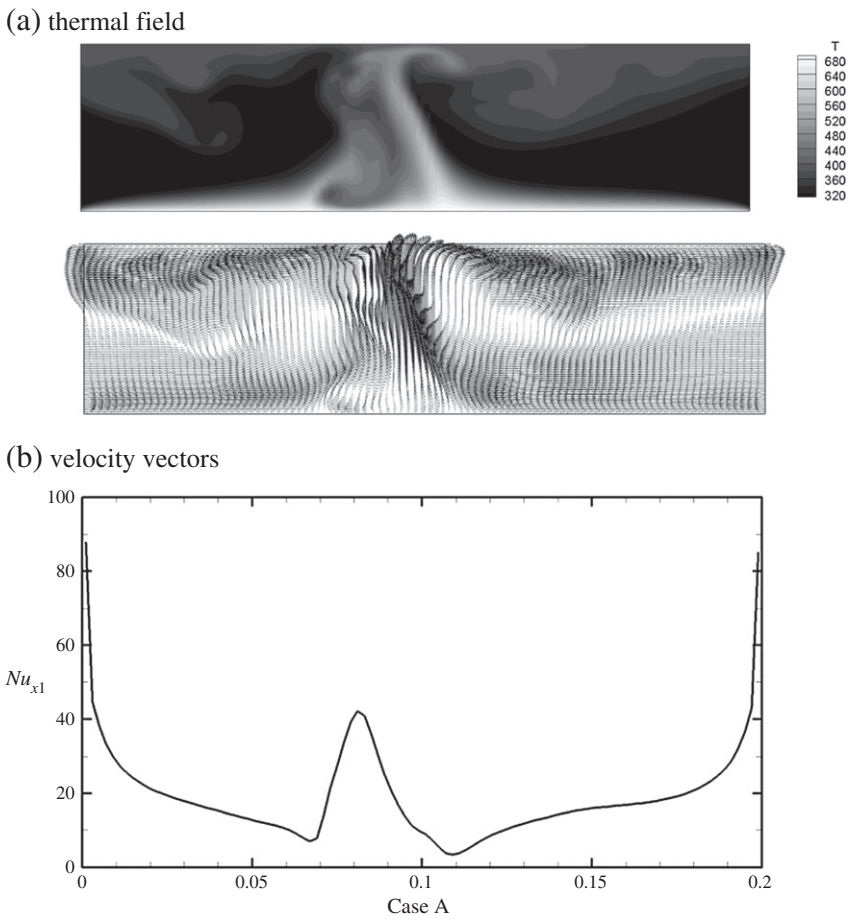

Fig. 4. Variations of a thermal field, velocity vectors and instantaneous local Nusselt numbers at a certain instant.

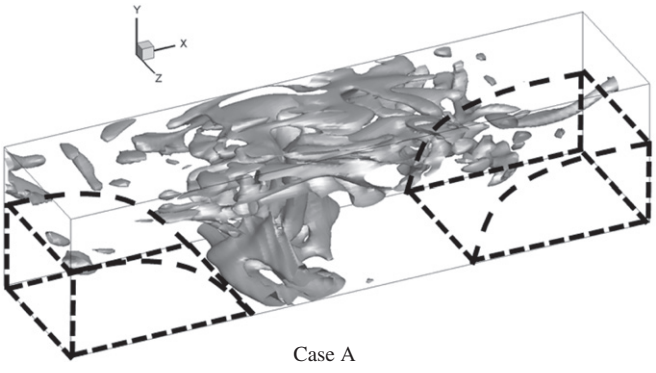

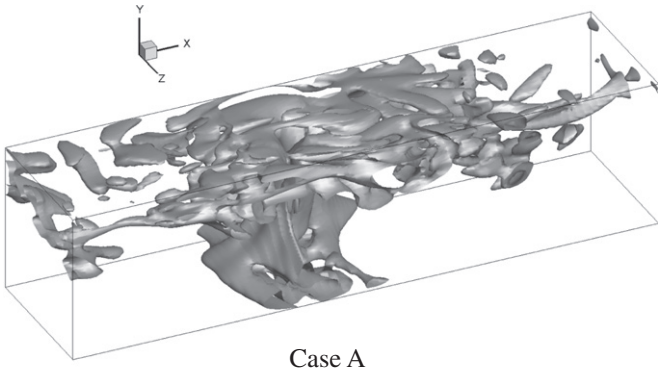

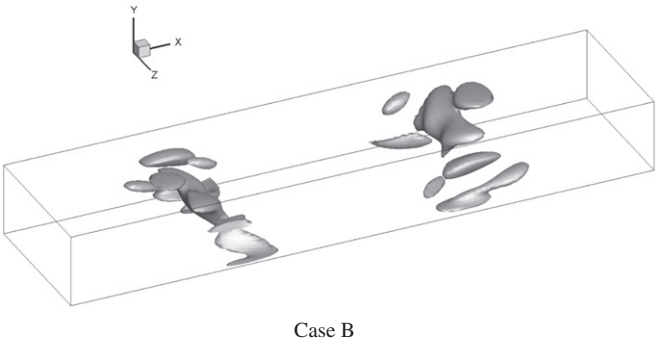

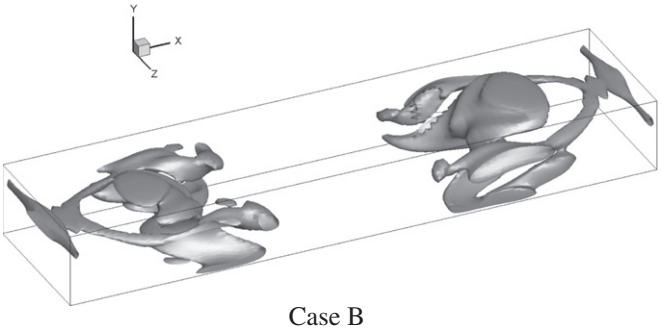

Fig. 5. Distributions of lumps of the iso-surface of the Q, Q = 500.

Fig. 6. Distributions of lumps of the iso-surface of the Q, Q = 300.

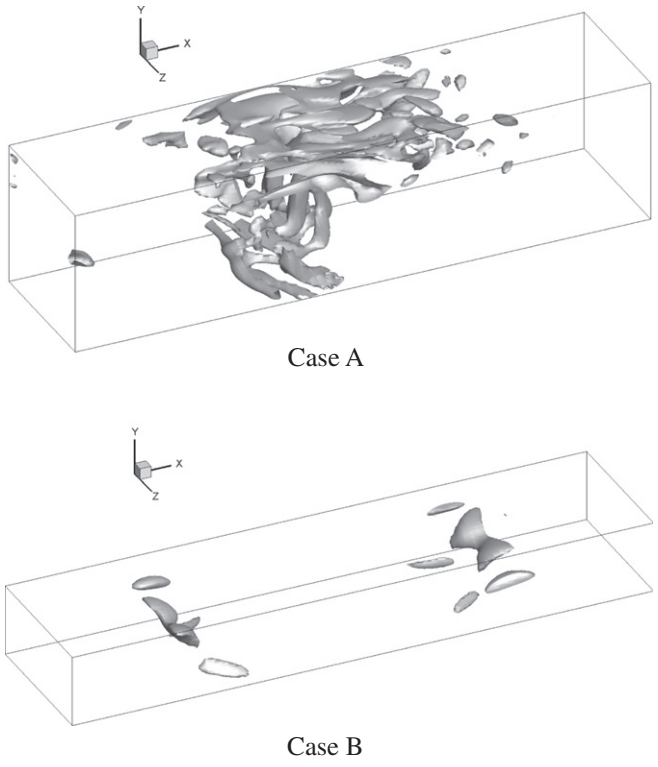

Fig. 7. Distributions of lumps of the iso-surface of the Q, Q = 1000.

6. Conclusions

An investigation of estimation of turbulent natural convection in horizontal parallel plates by the Q criterion is studied numerically. Rotation behaviors of natural convection indicated by the Q criterion are first displayed. Several conclusions are drawn as follows.

1. Due to the influence of the shear force in a low height situation, a few rotation structures are observed in the near central region where directions of flowing fluids are changed.
2. Rotation structures are almost fully filled with the space of a high height situation because of complete development of natural convection.
3. The Q criterion is a powerful method to be able to examine variations of rotation structures in a wide range.

Acknowledgment

The authors gratefully acknowledge the support of the Natural Science Council, Taiwan, R.O.C. under Contact NSC100-2221-E-009-086.

References

[1] S. Gavrilakis, Numerical simulation of low-Reynolds-number turbulent flow through a straight square duct, Journal of Fluid Mechanics 244 (1992) 101–129.
[2] D. Choi, C.L. Merkel, The application of preconditioning in viscous flows, Journal of Computational Physics 105 (1993) 207–223.
[3] B. Lessani, J. Ramboer, C. Lacor, Efficient large-eddy simulations of low Mach number flows using preconditioning and multigrid, Journal of Computational Physics 18 (2002) 221–233.
[4] M. Klein, A. Sadiki, J. Janicka, A digital filter based generation of inflow data for spatially developing direct numerical or large eddy simulation, Journal of Computational Physics 186 (2003) 652–665.
[5] W.S. Fu, C.G. Li, W.F. Lin, Y.H. Chen, Roe scheme with preconditioning method for large eddy simulation of compressible turbulent channel flow, International Journal for Numerical Methods in Fluids 61 (2009) 888–910.
[6] M. Miyamoto, H. Kajino, J. Kurima, I. Takanami, Development of turbulence characteristics in a vertical free convection boundary layer, Heat Transfer 2 (1982) 323–328.
[7] W.P. Jones, B.E. Lauder, The calculation of low Reynolds number phenomena with a two-equation model of turbulence, International Journal of Heat and Mass Transfer 16 (1973) 1119–1130.
[8] W.M. To, J.A.C. Humphrey, Numerical simulation of buoyant, turbulent flow—I. Free convection along a heated vertical plate, International Journal of Heat and Mass Transfer 25 (1987) 221–231.
[9] F.B. Cheung, D.Y. Sohn, Numerical study of turbulent natural convection in an innovative air cooling system, Numerical Heat Transfer Part A 16 (1989) 467–487.
[10] A.G. Fedorov, R. Viskanta, Turbulent natural convection heat transfer in an asymmetrically heated, vertical parallel- plate channel, International Journal of Heat and Mass Transfer 40 (1997) 3849–3860.
[11] J.R. Phillips, Direct simulations of turbulent unstratified natural convection in a vertical slot for Pr = 0.71, International Journal of Heat and Mass Transfer 39 (1996) 2485–2494.
[12] W.S. Fu, W.H. Wang, S.H. Huang, An investigation of natural convection of three dimensional horizontal parallel plates from a steady to an unsteady situation by a CUDA computation platform, International Journal of Heat and Mass Transfer 55 (2012) 4638–4650.
[13] J.C.R. Hunt, A.A. Wray, P. Moin, Eddies, Stream and Convergence Zones in Turbulent Flows, Report CTR-S88, Center for Turbulence Research, 1988.
[14] P.L. Roe, Approximation Riemann solver, parameter vectors, and difference schemes, Journal of Computational Physics 43 (1981) 357–372.
[15] J.M. Weiss, W.A. Simth, Preconditioning applied to variable and constants density flows, AIAA Journal 33 (1995) 2050–2056.
[16] S. Yoon, A. Jamesont, Lower–upper symmetric-Gauss–Seidel method for the Euler and Navier–Stokes equations, AIAA Journal 26 (1988) 1025–1026.
[17] W.S. Fu, C.G. Li, C.C. Tseng, An investigation of a dual-reflection phenomenon of a natural convection in a three dimensional horizontal channel without Boussinesq assumption, International Journal of Heat and Mass Transfer 53 (2010) 1575–1585.